หนึ่งอาจารย์หนึ่งผลงาน ประจำปีการศึกษา 2545

Manuscript entitled

"Functional reconstitution, gene isolation and topology modelling of porins from *Burkholderia pseudomallei* and *B. thailandensis*"

Siritapetawee, J., Prinz H., Samosornsook, W., Ashley R.H., and **Suginta W.**

The manuscript was submitted as a full paper to the Biochemical Journal

by

Dr. Wipa Suginta

School of Chemistry,
Suranaree University of Technology
Nakhon Ratchasima
Thailand

Functional reconstitution, gene isolation and topology modelling of porins from *Burkholderia pseudomallei* and *B. thailandensis*

Jaruwan SIRITEPTAWEE[*], Heino PRINZ[†], Worada SAMOSORNSUK[‡], Richard H. ASHLEY[§] and Wipa SUGINTA[*]

[*]School of Chemistry, Suranaree University of Technology, Nakhon Ratchasima 30000, Thailand; [†]Max Planck Institut für Molekulare Physiologie, Otto-Hahn-Strasse 11, 44227 Dortmund, Germany; [‡]Department of Medical Technology, Faculty of Allied Health Science, Thammasat University, Pathumthani 12120, Thailand; [§]Department of Biomedical Sciences, University of Edinburgh, George Square, Edinburgh EH8 9XD, Scotland, U.K.

Short title: *Burkholderia* porins

Keywords: diffusion pore, Omp38, *Burkholderia*, cloning, topology

Abbreviations used: FTIR, fourier transform infrared spectroscopy; MALDI-TOF, matrix-assisted laser desorption ionisation-time-of-flight; ESI/MS, electrospray mass spectrometry; MS/MS, tandem mass spectrometry; LPS, lipopolysaccharide, ECL, enhanced chemiluminescence, DTGS, deuterated triglycine sulphate; OM, outer membrane; MW, molecular weight; SEM, standard error of measurements.

Corresponding author:

Dr W SUGINTA, School of Chemistry, Suranaree University of Technology, Nakhon Ratchasima 30000, Thailand; tel: +66 44 224313; fax: +66 44 224185; email: wipa@ccs.sut.ac.th

Abstract

The intracellular pathogen *B. pseudomallei* is the causative agent of tropical melioidosis, and *B. thailandensis* is a closely-related gram negative bacterium that does not cause serious disease. Like other bacteria, their major outer membrane (OM) porins, *Bps*Omp38 and *Bth*Omp38, respectively, may have roles in antibiotic resistance and immunity. We purified both proteins and found them to be immunologically-related, SDS-resistant, heat-sensitive trimers of M_r ~110,000. In functional liposome swelling assays, both proteins showed similar permeabilities for small sugar molecules, compatible with a pore diameter of between 1.2 and 1.6 nm. Secondary structure analysis by FTIR revealed almost identical spectra with predominantly β-sheet structures, typical of bacterial porins. MALDI-TOF and ESI/MS analysis of each protein showed extensive sequence similarities to the OpcP1 porin from *B. cepacia* (later found to be 76.5% identical). Based on information from the incomplete *B. pseudomallei* genome sequencing project, the genes encoding Omp38 were identified and amplified by PCR from *B. pseudomallei* and *B. thailandensis* genomic DNA. The nucleotide sequences are 99.7% identical, and the predicted processed proteins are 100% identical. Topology prediction and molecular modelling suggest that this newly-isolated and cloned porin is a 16-stranded beta-barrel, and the external loops of the protein could be important determinants of the immune response to infection.

1. Introduction

Burkholderia pseudomallei (formerly *Pseudomonas pseudomallei*), the causative agent of tropical melioidosis, is a motile Gram-negative bacterium mainly endemic to Southeast Asia [1]. Although most cases are asymptomatic, the bacterium can cause acute, sub-acute or chronic illness [2], and acute septicaemias are often fatal within 48 hours, despite antibiotic therapy [3]. *B. thailandensis* is a closely-related non-pathogenic soil organism originally isolated in Central and North-East Thailand [4]. Although the two organisms are very similar [5,6], they are different in their genetic and biochemical properties. The rRNA sequence of *B. thailandensis* differs from that of *B. pseudomallei* by 15 nucleotides, and there are significant differences in genomic macrorestriction patterns between the organisms [7]. The biochemical profiles of these two species differ in that *B. thailandensis* utilises *L*-arabinose whereas *B. pseudomallei* does not [5,8]. *B. thailandensis* is also substantially less virulent in Syrian golden hamster models of infection [5].

The treatment of tropical melioidosis has in general proven to be extremely difficult. *B. pseudomallei* secretes a potent toxin that blocks protein synthesis in macrophages, although the organism itself can survive and multiply in these cells, as well as in phagocytes. The toxin may be responsible for the extensive abscess formation associated with the disease [9]. In addition, *B. pseudomallei* is resistant to many antibiotics including β-lactams, aminoglycosides, macrolides and polymyxins [1]. In some cases, this is because of their low permeability through the outer membrane of the bacteria [10]. Given that these hydrophilic molecules often diffuse through water-filled porins [11], the characteristics of specific porin channels may be significant determinants of antibiotic sensitivity [10,11]. In conjunction with peptidoglycan and lipopolysaccharide (LPS), porins are also receptors for bacteriophages and bacteriocidins, and they also have a significant structural role in maintaining the integrity of the cells [12].

Porins had been identified in many Gram-negative bacteria [13-20], and several porins from *Escherichia coli* (OmpF, OmpC, and PhoE) have been well characterised in terms of their biochemical, functional, genetic, immunochemical, and structural properties [21-23]. In particular, all porins appear to contain abundant β-sheet structures [24,25]. The OM of the related organism *B. cepacia* (responsible for fatal lung infections in cystic fibrosis) contains an 81-kDa porin designated OpcP0, which also shows low permeability to β-lactams [26]. This protein contains two subunits: a major 36-kDa protein designated OpcP1, and a minor 27-kDa protein, designated OpcP2. OpcP1 has been cloned and expressed in *E. coli* [27]. The

predicted OpcP1 protein precursor contains 361 residues, including a 20-residue signal sequence. The calculated M_r of 35,696 for the mature protein is in agreement with the OpcP1 protein band of 36 kDa on SDS-PAGE. Homology of the amino acid sequences between OpcP1 and several other Gram-negative bacterial porins strongly suggests that OpcP1 is the pore-forming component of OpcP0. This notion is also supported by the similarity of the hydropathy plots of OpcP1 and the major *E. coli* porin, OmpF [26].

Like chlamydial porins [28], *Burkholderia* (including *B. pseudomallei*) porins may also provide important vaccine targets, especially if their structures can be elucidated to guide the generation of protein or DNA-based vaccines. It may also be possible to generate live attenuated organisms containing modified porins, to elicit active immunity. In this study, we describe the isolation of *Bps*Omp38 from *B. pseudomallei* and *Bth*Omp38 from *B. thailandensis*, and characterise them using FTIR spectroscopy and MALDI-TOF MS and nanoESI/MS. Peptide mass fingerprinting showed the amino acid sequences of the proteins to be identical, and enabled us to identify and isolate the gene encoding *Bps*Omp38 from the partially-sequenced *B. pseudomallei* genome. We have also cloned its homologue from *B. thailandensis* genomic DNA, and the predicted proteins have been subjected to topology prediction and structural modelling.

2. Experimental

2.1 Materials.

Bacteria culture media and bacteriological agar were purchased from Scharlau Chemie (Spain). Cetyltrimethylammonium bromide (CTAB), dithiotreitol (DTT), iodoacetamide, ammonium hydrogen carbonate, *D*-stachyose, *D*-melezitose, *D*-sucrose, *L*-arabinose, *D*-glucose and *D*-mannose were from Acros Organics (USA). Proteinase K and trypsin (sequencing grade) were from Promega (USA). Sephacryl S-200® HR resin and Dextran T-40 were from Amersham Pharmacia Biotech (Sweden). Detergents used for protein preparation were purchased from Carlo Erba Reagenti (Italy). All other reagents for general laboratory uses were from Sigma-Aldrich (Germany) and Carlo Erba Reagenti (Italy). *Taq* DNA polymerase was purchased from Promega (USA). Primers for PCR amplification were synthesised by Proligo Singapore Pty Ltd (Singapore).

2.2 *Preparation of OM proteins.*

B. pseudomallei (ATCC 23343) and *B. thailandensis* (ATCC 700388) were grown in LB broth at 37°C with vigorous shaking. Cells were harvested at late exponential phase by centrifugation at 10,000 x g at 4°C for 20 min. Crude peptidoglycan was isolated using a

modification of the method of Gotoh *et al.* [29]. Briefly, cells from 2 l of late exponential culture were washed once and suspended in 10 ml of 10 mM Tris-HCl, pH 8.0 containing 1 mM PMSF and 2 mg hen egg lysozyme. The suspension was sonicated using a Sonopuls Ultrasonic homogenizer with a 6 mm diameter probe (50% duty cycle; amplitude setting 20%; total time 5 min), and large cellular debris and unbroken cells were removed by centrifugation at 10,000 x g for 30 min. Cell membranes were recovered from the lysates by microcentrifugation at 12,000 x g for 1 h, suspended in 10 mM Tris-HCl, pH 8.0 containing 0.5% (w/v) SDS, and heated at 30°C for 1 h to solubilise most of the remaining cytoplasmic and membrane proteins. A complex of non-solubilised peptidoglycan sheets (crude peptidoglycan) was then pelleted by microcentrifugation at 12,000 x g for 1 h and heated in 4 ml of 10 mM Tris-HCl, pH 8.0 containing 2% (w/v) SDS and 0.5 M NaCl at 37°C for 1 h. Solubilised peptidoglycan-associated proteins were then separated from insoluble peptidoglycan by microcentrifugation at 12,000 x g for 1 h.

2.3 Proteoliposome swelling assay.

The preparation of proteoliposomes and the determination of diffusion rates were based on the detailed methods described previously [29-31]. Briefly, mixtures of 2.4 μmol phosphatidylcholine and 0.2 μmol dicetylphosphate in chloroform were dried by vacuum centrifugation and the phospholipid films were resuspended in 0.2 ml distilled water and mixed with 50 μg purified outer membrane protein. The mixtures were sonicated for 7 min in a water bath at 20°C, dried overnight by vacuum centrifugation, and resuspended in 0.2 ml of 10 mM Tris-HCl, pH 8.0 containing 15% (w/v) Dextran T-40, to form proteoliposomes. The proteoliposomes were diluted into 0.6 ml of an isoosmotic sugar solution (prepared as described in the Results section), and changes in absorbance were measured at 400 nm for 60 s. The relative permeabilities of the pore-forming proteins were assumed to be proportional to the initial swelling rates [32], and each experiment was repeated at least three times using liposomes without any protein, or liposomes containing bovine serum albumin, as negative controls.

2.4 Immunological analysis and SDS-PAGE.

Purified *B. pseudomallei* Omp38 (2 μg) was separated by SDS-PAGE as a monomer using 12% (w/v) acrylamide and 8 M urea in a Laemmli buffer system [33]. Following electrophoresis, the protein was stained with Coomassie blue. After destaining, the protein band was excised from the gel, emulsified with 50 μl Freund's complete adjuvant (Pierce), and used to raise rabbit polyclonal antiserum [34]. Antisera titres and cross reactivity between

B. pseudomallei and *B. thailandensis* proteins (each 5 μg) were analysed by Western blotting with enhanced chemiluminescence (ECL®, Amersham Pharmacia Biotech) detection, using 1:10,000 dilutions of the anti-Omp38 antiserum in phosphate buffered saline, pH 7.4 in the presence of 0.2% (v/v) Tween 20 and 5% (w/v) non-fat dried milk. Protein concentrations were determined using a BCA kit (Pierce).

2.5 Protein identification and peptide mass analysis by MALDI-TOF MS and ESI/MS.

Protein identification was performed in two steps: For the initial analysis, the protein bands from SDS-gels (see above) were excised, destained, reduced, alkylated with iodoacetamide and digested with sequencing grade trypsin (Promega) following a standard protocol [35]. After overnight digestion at 37°C, the peptides were extracted and dried in a SpeedVac vacuum centrifuge. A small fraction of these tryptic peptides was analysed by MALDI-TOF MS (Voyager-DE Pro in reflective mode) in an α-cyano-4-hydroxycinnamic acid matrix for the peptide "mass fingerprinting". The remaining peptides were separated by capillary HPLC using a 0-40% linear gradient of acetronitrile containing 0.1% acetic acid, then detected directly by ESI/MS (Thermo Finnigan LCQ Deca) using the proprietary "triple play" mode for obtaining MS/MS sequence information for the relevant peptides. Data bank searching was performed with "MS-Fit" (http://prospector.ucsf.edu/) for MALDI mass fingerprint data, and with "Sequest search" (http://fields.scripps.edu/sequest/index.html) for MS/MS data from the HPLC-MS run. In some experiments, the proteins (not gel pieces) were completely digested with sequencing grade Trypsin in a buffer containing 5 mM $CaCl_2$ and 100 mM NH_4HCO_3, and the resulting peptides were applied to an Agilent 1100 HPLC connected to the LCQ ESI/MS. Mass spectra of whole proteins were obtained with linear MALDI-TOF (Voyager-DE Pro) using sinapinic acid (3,5-dimethoxy-4-hydroxycinnamic acid) as the matrix.

2.6 FTIR measurements.

FTIR measurements were carried out using a Bruker IFS-66 FTIR spectrometer equipped with a DTGS detector. The protein solutions (5 μl, 10 mg/ml) were placed in home-made demountable cells with CaF_2 windows with a path length of 84 μm. The samples were dried *in vacuo* for 5 min and analysed in ^1H_2O (5 μl). To compensate for ^1H_2O absorption, buffer solutions alone were subtracted using the same cells. FTIR spectra of the protein solutions were recorded using identical scanning parameters. Typically, the resolution was set to 4 cm^{-1} and 34 scans were accumulated before performing a Fourier-transform analysis to optimise the signal-to-noise ratio. The protein spectrum was obtained after subtracting the buffer

spectrum from the spectrum of the protein solution measured under the same conditions. To eliminate spectral contributions due to atmospheric water vapour, the instrument was continuously purged with dry air. Spectral contributions from residual water were eliminated using water vapour spectra measured under identical conditions. The absorption region 1000 to 4000 cm^{-1} was primarily monitored. However, to obtain secondary structural components of the proteins, the amide I absorption region 1500 to 1800 cm^{-1} was specifically acquired for second derivative plots.

2.7 Preparation of genomic DNA and cDNA cloning and sequencing.

Genomic DNA was prepared using the protocol of Ausubel *et al.* [36]. PCR primers were synthesised by Proligo Genset (Singapore). Amplification reactions were carried out using *Taq* polymerase and the products were cloned into pGEM®-T vector and sequenced in both directions using an automated sequencer (Biotechnology Sequencing Unit (BSU), Thailand).

2.8 Structural prediction and molecular modelling.

Protein sequences were aligned using ClustalW (http://www.ebi.ac.uk/clustalw/) and displayed using Genedoc (http://www.psc.edu/biomed/genedoc/). Signal peptide cleavage sites were predicted using SignalP V1.1 (http://www.cbs.dtu.dk/services/SignalP/) and transmembrane domains were predicted using prediction of the protein localisation sites (http://psort.ims.u-tokyo.ac.jp/cgi-bin/okumura.pl). RPS-BLAST (http://www.ncbi.nih.gov./BLAST) was used to identify conserved domains, and protein structures were modelled and displayed using 3D-PSSM (http://www.sbg.bio.ic.ac.uk/~3dssm), 123D+ search (http://123d.ncifcrf.gov), and Swiss-Model (http://www.expasy.org/swissmod).

3. Results

3.1 Purification of BpsOmp38 and BthOmp38 porins.

Crude peptidoglycan isolated from *B. pseudomallei* and *B. thailandensis* (see Methods) was used as the starting material to purify trimeric outer-membrane proteins (Omps). Following SDS extraction, the peptidoglycan fraction was further purified by size-exclusion chromatography (200 ml Sephacryl S-200® HR column) in the presence of 1% (w/v) SDS and 0.5 M NaCl. Eluted protein was detected by measuring the absorbance of the eluate at 280 nm, and peak fractions were analysed by 12.5% (w/v) SDS-PAGE in the presence of urea [23].

Fig. 1 near here

For each organism, the major protein peak obtained after size-exclusion chromatography (Fig. 1A) corresponded to a M_r of ~100,000. As shown in Fig. 1B, this relatively high molecular weight band shifted to M_r ~38,000 after heating at 95°C for 5 min. Taken together, the results from size exclusion chromatography and SDS-PAGE suggested that the isolated proteins were SDS-resistant homotrimers comprised of M_r ~38,000 monomers, consistent with trimeric OM porins. Similar results were seen in 10 independent preparations. The proteins isolated from *B. pseudomallei* and *B. thailandensis* were therefore designated *Bps*Omp38 and *Bth*Omp38, respectively. The final yield of each protein obtained from a 2-l culture was approximately 0.2% (800 μg and 600 μg for *B. pseudomallei* and *B. thailandensis*, respectively) (Table 1).

Table 1 near here

3.2 Antibody production and immunoblotting analysis.

The protein band corresponding to the *B. pseudomallei* Omp38 monomer was excised from a gel and used to raise a rabbit polyclonal antiserum as described under Methods. The antibodies cross reacted with both proteins on immunoblots, and also recognised the high-MW, presumed trimeric, protein band in non-denatured samples. In addition, the antibodies also recognised a 39,000 protein from *E. coli* BL21(DE3) OM fraction. None of these proteins was recognised by rabbit pre-immune serum (not shown), suggesting that the *Burkholderia* proteins may be structurally related to at least one *E. coli* porin.

Fig. 2 near here

3.3 Secondary structure analysis using FTIR.

The second derivative plots obtained from FTIR measurements revealed extensive secondary structure similarity between *Bps*Omp38 and *Bth*Omp38, and their spectra could almost be directly superimposed apart from minor differences in the regions associated with turns & loops (IR bands 1651.5 cm^{-1} and 1673.7 cm^{-1}) and lipopolysaccharide (IR bands 1727.4 cm^{-1} and 1740.1 cm^{-1}) (Fig. 3) [37]. It was noticeable that *Bps*Omp38 contained more associated LPS than *Bth*Omp38. The secondary derivative plots in the amide I (1500 to 1800 cm^{-1})

region demonstrated that both proteins contained predominantly β-sheet, as shown in the two distinct peaks at 1626.3 cm^{-1} representing major β–sheet components and 1695.9 cm^{-1} representing anti-parallel β–sheets. Only minor contributions from α-helices (1650.0 cm^{-1}) and loops and turns (1651.5 cm^{-1} and 1673.7 cm^{-1}) were observed. Taken together, these secondary structure features are typical of porins [25,38].

Fig 3 near here

3.4 Liposome swelling assay.

Our data strongly suggested that *Bps*Omp38 and *Bth*Omp38 were likely to be porins, and that they had been isolated in a non-denatured, possibly native, conformation. In particular, both membrane proteins retained significant secondary and quaternary structures (comprising mainly β-sheet, and SDS-resistant, heat-sensitive trimers, respectively). The apparent retention of normal folding suggested that they might form functional channels, and we tested this idea by assaying solute transport in liposome swelling assays.

Following reconstitution, the relative diffusion rates of *L*-arabinose, *D*-glucose, *D*-mannose, *D*-galactose, *N*-acetylglucosamine, *D*-sucrose and *D*-melezitose into multilamellar liposomes were determined as described in the Methods section, after establishing "isosmotic" buffer conditions in the presence of the large impermeant sugar, stachyose (667 Da). Absorbance changes for each sample were positive, and increased linearly with time from the outset of each recording (not shown), confirming that the starting conditions were isosmotic and the proteoliposomes were properly equilibrated. The diffusion rates of all the sugars we tested increased linearly with [protein] (Fig. 4A and 4B), and the rates clearly depended on the M_r of the solute.

Fig. 4 near here

As shown in Fig. 4C, the relative diffusion rates through *Bps*Omp38 and *Bth*Omp38 porins were indistinguishable, with a "limiting" M_r of ~650 (defined as the value corresponding to 5% relative permeability). The rates were clearly different from the rates through *E. coli* OM porin (mainly OmpF, under the growth conditions used) which, when reconstituted under exactly the same conditions, had a limiting M_r of ~450 (data not shown).

3.5 Gene isolation, cloning and sequencing.

We analysed the primary structures of *Bps*Omp38 and *Bth*Omp38 in order to identify the corresponding genes from genome sequences. As identified by MALDI-TOF MS, the masses of *Bps*Omp38 and *Bth*Omp38 were 37,159 and 37,108, respectively. This is identical within the weight dependent peak broadening of MALDI-TOF protein measurements. MALDI mass fingerprints of tryptic fragments obtained from in-gel digests revealed almost identical peptide ensembles. When these peptides were separated on a capillary HPLC and subjected to partial fragmentation (ESI-MS/MS sequence analysis), eight *Bps*Omp38 peptides (TDVYAQAVYQR, GSEDLGGGLK, SLWSVGAGVDQSR, LNTNGDVAVNNTVK, AYSAGASYQFQGLK, QAFVGLSSNYGTVTLGR, AIFTLESGFNIGNGR, and NANASIYNGDLSTPFSTSINQTAATVGLR) and four identical *Bth*Omp38 peptides (GSEDLGGGLK, SLWSVGAGVDQSR, QAFVGLSSNYGTVTLGR, and AIFTLESGFNIGNGR) gave an unambiguous match to the outer membrane porin OpcP1 of *B. cepacia.* Each of these peptides could also be aligned with a single predicted ORF in contig 836 of the *B. pseudomallei* genome (http://www.ncbi.nlm.nih.gov/sutils/genom_table.cgi).

Fig. 5 near here

Accordingly, we amplified full-length *Bps*Omp38 and *Bth*Omp38 cDNAs, each containing 1,112 nt, from appropriate genomic DNA using the following sense primer: 3'-ATGAACAAGACTCTGATTGTTGCA-5', and antisense primer: 3'-GAAGCGGTGACGCAGACCAA-5' using *Taq* DNA polymerase. The cDNAs were cloned into pGEM®-T vector (Promega) and transformed into *E. coli* host strain DH5∝. The sequences of both inserts were determined [39] and have been deposited in GeneBank (AY312416 and AY312417 for *Bps*Omp38 and *Bth*Omp38, respectively). The DNA sequences were >98% identical, with no codon changes (not shown). When these sequences were used to calculate the masses of our tryptic peptides, we could identify almost every peptide from the prior HPLC-MS analysis (Fig 5). As expected, the exceptions were peptides containing fewer than four amino acid residues. The first amino acid detected by HPLC-MS was Ala^{41} and the last was (as expected) Arg^{371}. The peptide composition as analysed by HPLC-MS was identical for both proteins.

3.6 Protein structure prediction.

SignalP was used to predict Omp38 signal sequences, and when these were removed the calculated M_r of the identical, processed, leaderless proteins was 37,163.5. This value agrees well with the estimate from MALDI-TOF analysis of the purified proteins. The predicted amino acid sequences of the preproteins were next analysed for homology with *Burkholderia* and other Gram-negative bacterial porins (Fig. 6). The membrane topology of Omp38 was predicted by the

Fig 6 near here

method of Diederichs et al. [40], and the 3D structure of the protein was analysed using 123D+ and Swiss-Model. Omp38 had most similarity to the anion selective porin Omp32 (PDB 1e54a), (35.8% identity when using Swiss-Model). The predicted topology of 16 transmembrane domains, 8 loops and 8 periplasmic turns is compatible with a 16-stranded porin beta barrel in which the *N*-terminus forms a salt bridge with the *C*-terminus immediately after a periplasmic turn, and based on both transmembrane topology prediction and 3D structure modelling, Omp38 has a β-barrel structure with 16 transmembrane strands, eight short periplasmic turns and 8 external loops (Fig. 7). The longest loop, Loop 3 ($Ser^{127} \rightarrow Asp^{154}$), contains two short, antiparallel β strands at the very beginning and the end of the loop, and a short right-handed α helix ($Tyr^{119} \rightarrow Lue^{126}$) was found to precede the long loop 3. This loop is characteristic of many porins as a pore-confined loop responsible for the size selectivity of the channel [41].

Fig. 7 near here

4. Discussion

Porins play crucial roles in the interactions between Gram-negative bacteria and their environment. In this study, we purified and characterised the major outer membrane porin of the pathogenic bacterium, *Burkholderia pseudomallei*, and the equivalent porin from the closely-related non-pathogenic bacterium, *B. thailandensis*. When the oligomeric proteins (M_r 110,000) were heated to 95°C, they disassociated into M_r 38,000 monomers. This process was irreversible, and it has been suggested that on heating porin β-sheets are converted into α-helices [42,19], preventing reassemble into trimers.

When reconstituted in liposomes for functional analysis, the results were consistent with those expected for "general diffusion" porins [22,23]. Although the highest diffusion rate corresponded to the smallest sugar, *L*-arabinose (150 Da), *D*-glucose (180 Da) permeated measurably faster than other sugars with the same molecular weight (*D*-mannose and *D*-galactose). *B. pseudomallei* and *B. thailandensis*, like other Gram-negative bacteria, utilise glucose as a primary source of carbon for cell growth, and enhanced glucose permeation may be functionally significant. *B. thailandensis* can utilise *L*-arabinose, while *B. pseudomallei* cannot [5]. However, the relative diffusion rates of *L*-arabinose was the same (Fig. 2), suggesting that Omp38 is not a sugar-specific channel for *L*-arabinose. The diameter of the 38-kDa porin protein can be estimated to be between 1.2-1.6 nm, on the basis of very similar sugar permeability when compared to the 42-kDa porin of *S. liqueaciens* [32].

FTIR analysis showed that Omp38 contained predominantly β strands and was likely to form an antiparallel β-barrel characteristic of bacterial OM porins [43-45]. The IR patterns of both proteins were almost identical with slight differences found in the turn & loop and lipopolysaccharide regions. It is not known whether this may be reflected in genuine differences in the final conformations of the otherwise identical proteins. The analysis also showed that Omp38 preparations always contained varying amount of LPS. Although both were isolated and purified by the same procedure, *Bps*Omp38 contained higher amount of LPS than *Bth*Omp38 (Fig. 3). The data in Fig. 1B also suggest the presence of LPS in the purified proteins, with a "ladder" of several bands in the unheated samples (*cf* Eisele and Rosenbusch) [46]. The idea of a strong porin-LPS interaction is supported by the fact that solubilisation of Omp38 by a strong detergent (SDS) and gel-filtration failed to remove the LPS completely. However, for immunoblot, MS and liposome swelling assays, complete removal of LPS is not required.

We isolated the gene encoding Omp38 gene from *B. pseudomallei* and *B. thailandensis* genomic DNA after identifying the genes following protein MS analysis. We found that almost all the back-translated amino acid sequences of both organisms could be matched to peptide fragment data from capillary HPLC-ESI/MS of the native porins (Fig. 5). Some amino acid sequences in the mature proteins could not be identified using HPLC-ESI/MS. At high concentrations, membrane proteins tend to aggregate, and this might hinder analysis by HPLC-ESI/MS and MALDI-MS [47]. Our prior immunoblot analysis (Fig. 2) had already suggested that *Bps*Omp38 and *Bth*Omp38 are homologous or identical, and the antiserum also cross-reacted with *E. coli* porin (OmpF).

Omp38 is one of a large number of porins that usually form trimers and have individual subunits that fold into 16 or 20-stranded barrels. Topology and 3D-prediction programs strongly suggest that Omp38 folds as a 16-stranded barrel with 8 loops and 8 turns, with closest similarity the anion-selective porin from *Comamonas acidovorans* [41]. The longest loop (L3) folds into the barrel. This loop, which contains a short α-helix, constricts the size of the pore of the barrel. L8, which is the second longest loop, also folds into the barrel interior and contributes to the formation of the particularly narrow external channel opening.

To our knowledge, this is the first time that a porin of 38 kDa has been isolated from *B. thailandensis*, and have its sequence, secondary structure and activity analysed. We have cloned and sequenced the genes encoding Omp38 porins from both *B. thailandensis* and *B. pseudomallei*, and shown the proteins to be identical. Further work is underway to determine the importance of Omp38 in antibiotic resistance and immunity, and to determine its 3D-structure by protein crystallisation and X-ray diffraction.

Acknowledgements

This work was supported by a Suranaree University of Technology Grant (grant number: SUT-106-46-36-02), by a Shell Studentship to Miss Jaruwan Siritapetawee, by a grant from the German Academic Exchange Service "DAAD" (to WS), and by the Wellcome Trust (to RHA). We would like to thank Prof. Dieter Naumann, Robert-Koch Institute, Berlin, Germany for help with FTIR measurements and Dr. Albert Schulte, Ruhr University of Bochum, Germany, for his advice on the manuscript.

References

1 Moor, R. A. , DeShazer, D., Reckseidler, S., Weissman, A. and Woods, D. E. (1999). Efflux mediated aminoglycoside and macrolide resistance in *Burkholderia pseudomallei*. Antimicrob. Agents Chemother. **43**, 465-470

2 Brown, N. F. and Beacham, I. R. (2000). Cloning and analysis of genomic differences unique to *Burkholderia pseudomallei* by comparison with *B. thailandensis*. Med. Microbiol. **49**, 993-1001

3 Guard, R.W., Khafagi, F.A., Rigden, M.C. and Ashdown, L.R. (1984) Melioidosis in Far North Queensland,. A clinical and epidemiological review of twenty cases. Am. J. Trop. Med. Hyg. **33**, 467-473

4 Brett, P. J., DeShazer, D. and Woods, D. E. (1997). Characterization of *Burkholderia pseudomallei* and *Burkholderia pseudomallei*-like strains. Epidemiol. Infect. **118**, 137-148

5 Brett, P. J., DeShazer, D. and Woods, D. E. (1998) *Burkholderia thailandensis* sp. Nov., description of a *Burkholderia pseudomallei*-like species. In. J. Syst. Bacteriol. **48**, 317-320

6 Yabuuchi, E., Kosako, Y., Oyaizu, H., Yano, I., Hotta, H., Hashimoto, Y., Ezaki, T and Arakawa, M.(1992). Proposal of *Burkholderia* gen. Nov. and transfer of seven species of the genus *Pseudomonas* homology group 11 to the new genus, with the type species *Burkholderia cepacia* (Palleroni and Homlmes 1981) comb. Nov. Microbiol. Immuno. **36,** 1251-127

7 Chaiyaroj, S. C., Kotrnon, K., Koonpaew, S., Anantagool, N., White, N. J. and Sirisinha., S. (1999) Differences in genomic macrorestriction patterns of arabinose-positive (*Burkholderia thailandensis*) and arabinose-negative *Burkholderia pseudomallei* Microbiol. Immunol.**43**, 625-630

8 Wuthiekanun, V., Smith, M. D., Dance, D. A., Walsh, A. L., Pitt, T. L. and White, N. J. (1996) Biochemical characteristics of clinical and environmental isolates of *Burkholderia pseudomallei* J. Med. Microbiol. **45**, 408-412

9 Gridley, D. S. (1999) Non-fermenting aerobic Gram-negative *bacilli.* In Essentials of diagnostic microbiology. (Shimeld, L. A., ed.), pp. 206-221, Delmar Publishers, New York

10 Bianco, N., Neshat, S. and Poole, K. (1997) Conservation of the multidrug resistance efflux gene oprM in *Pseudomonas aeruginosa.* Antimicrob. Agents Chemother. **41**, 853-856

11 Hancock, R. E. W. (1987) Role of porins in outer membrane permeability. J. Bacteriol. **169**, 929-933

12 AlbertÍ, S., RodrÍquez-quiñones, F., Schirmer, T., Rummel, G., Tomas, J. M., Rosenbusch, J.P. and BenedÍ, V. J. (1995) A porin from *Klebseilla pneumoniae*: sequence homology, three-dimensional model, and complement binding. Infect. Immun. **63**, 903-910

13 Hancock, R. E. W., Decad, G. M. and Nikaido, H. (1979) Identification of the protein producing transmembrane diffusion pores in the outer membrane of *Pseudomonas aeruginosa* PAO1. Biochem. Biophys. Acta. **554**, 323-331

14 Douglas, J. T., Lee, M. D. and Nikaido, H. (1981) Protein I of *Neisseria gonorrhoeae* outer membrane is a porin. FEMS Microbial Lett. **12**, 305-309

15 Darveau, R. P., MacIntyre, S., Buckley, J. T. and Hancock, R. E. W. (1983) Purification and reconstitution in lipid bilayer membranes of an outer membrane, pore-forming protein of *Aeromonas salmonicida*. J. Bacteriol. **156**, 1006-1011

16 Bavoil, P., Ohlin, A. and Schachter, J. (1984) Role of disulfide bonding in outer membrane structure and permeability in *Chlamydia trachomatis*. Infect. Immun. **44**, 479-485

17 Douglas, J. T., Rosenberg, E. Y., Nikaido, H., Verstreate, D. R. and Winter, A. J. (1984) Porins of *Brucella* species. Infect. Immun. **44**, 16-21

18 Flammann, H. and Weckesser, J. (1984) Porin isolated from the cell envelope of *Rhodopseudomonas capsulata*. J. Bacteriol. **159**, 410-412

19 Weckesser, J., Zalman, L. S. and Nikaido, H. (1984) porin from *Rhodopseudomonas sphaeroides*. J. Bacteriol. **159**, 199-205

20 Gotoh, N., Wakebe, H., Yoshihara, E., Nakae, T. and Nishino, T. (1989) Role of protein F in maintaining structural integrity of the *Pseudomonas aeruginosa* outer membrane. J. Bacteriol. **171**, 983-990

21 Rocgue, W. J. and McGroarty, E. J. (1989) Isolation and preliminary characterization of Wild-type OmpC porin dimers from *Escherichia coli* K-12. Biochemistry **28**, 3738-3743

22 Cowan, S. W. (1993) Bacterial porins: lessons from three high-resolution structures. Curr. Opin. Struct. Biol. **3**, 501-507

23 Nikaido, H. (1994) Porins and specific diffusion channels in bacterial outer membrane permeability. Microbiol. Rev. **49**, 1-32

24 Nikaido, H. and Vaara, M. (1985). Molecular basis of bacterial outer membrane permeability. Microbiol. Rev. **49**, 1-32

25 Brunen, M., Engelhardt, H., Schmid, A. and Benz, R. (1991) The major outer membrane protein of *Acidovorax delafieldii* is an anion-selective porin. J. Bacteriol. **173**, 4182-4787

26 Gotoh, N., Nagino, K., Wada, D., Tsujimoto, H. and Nishino, T. (1994) *Burkholderia* (formerly *Pseudomonas*) *cepacia* porin is an oligomer composed of two component proteins. Microbiology. **140**, 3285-3291

27 Tsujimoto, H., Gotoh, N., Yamagishi, J., Oyamada, Y. and Nishino, T. (1997) Cloning and expression of the major porin protein gene *opc*P of *Burkholderia* (formerly *Pseudomonas cepacia*) in *Escherichia coli*. Gene **186**, 113-118

28 Wolf, K., Fischer, E., Mead, D., Zhong, G., Peeling., R., Whitmire, B. and Caldwell, H.D.,(2001) *Chlamydia pneumoniae* major outer membrane protein is a surface-exposed

antigen that elicits antibodies primarily directed against conformation-dependent determinants. Infect Immun. **69**, 3082-3091

29 Gotoh, N., White, N. J., Chaowagul, W. and Woods, D. (1994) Isolation and characterization of the outer-membrane proteins of *Burkholderia* (*Pseudomonas*) *pseudomallei*. Microbiology. **140**, 797-805

30 Nikaido, H. and Rosenberg, E. Y. (1983) Porin channels in *Escherichia coli*: studies with liposomes reconstituted from purified proteins. J. Bacteriol. **153**, 241-252

31 Yoshimura, F., Zalman, L. S. and Nikaido, H. (1983) Purification and properties *Pseudomonas aeruginosa* porin. J. Biol. Chem. **258**, 2308-2314

32 Nitzan, Y., Orlovsky, K. and Pechatnikov, I. (1999) Characterization of porins isolated from the outer membrane of *Serratia liquefaciens*. Curr. Microbiol. **8**, 71-79

33 Arckiasamy, A. and Krishnaswamy, S. (2000) Purification of integral outer-membrane protein OmpC, a surface antigen from *Salmonella typhi* for structure-function studies: a method applicable to enterobacterial major outer-membrane protein. Anal. Biochem. **283**, 64-70

34 Amero, S. A., James, T. C. and Elgin, S. C. R. (1994) Production of antibodies using proteins in gel bands. In Basic protein and peptide protocols. (Walker, J. M., ed.), pp. 401-406, Humana Press, New Jersey

35 Shevchenko, A.; Wilm, M.; Vorm, O. and Mann, M., (1996) Mass spectrometric sequencing of proteins silver-stained polyacrylamide gels. Anal.Chem. **68**, 850-858

36 Ausubel, F. M., Brent, R., Kingston, R. E., Moore, D. D., Smith. J. A. and Strukh, K. (1999) Short Protocols in Molecular Biology,. 4th edition, pp.2-12, Wiley & Sons, New York

37 Mäntele, W. and Fabian, H. (2002) Infrared Spectroscopy of Proteins In Handbook of Vibrational Spectroscopy (Chalmers, J.M. and Griffiths, P.R., ed.), pp. 1-27, John Wiley & Sons, Chichester

38 Abrecht, H., Goormaghtigh, E., Ruysschaert, J.M., Homble, F. (2000) Structure and orientation of two voltage-dependent anion-selective channel isoforms. An attenuated total reflection fourier-transform infrared spectroscopy study. J. Biol. Chem. **275**, 40992-40999

39 Sanger, F., Nicklen, S. and Coulson, A. R. (1977) DNA sequencing with chain-terminating inhibitors. Proc. Natl. Acad. Sci. U S A. **12**, 5463-5467

40 Diederichs, K., Freigang, J., Umhau, S., Zeth., K. and Breed, J. (1998) Prediction by aneural network of outer membrane beta-strand protein topology. Protein Sci. **7**, 2413-2420

41 Zeth, K., Diederichs, K., Welte, W. and Engelhardt, H. (2000) Crystal structure of Omp32, the anion-selective porin from *Comamonas acidovorans*, in complex with a periplasmic peptide at 2.1 Å resolution. Structure. **8**, 981-992

42 Tokunaga, M., Tokunaga, H., Okajima, Y. and Nakae, T. (1979) Characterization of porins from the outer membrane of *Salmonella typhimurium* 2. Physical properties of the functional oligomeric aggregates. Eur. J. Biochem. **95**, 441-448

43 Forst, D., Welte, W., Wacker, T. and Diederichs, K. (1998) Structure of the sucrose-specific porin ScrY from *Salmonella typhimurium* and its complex with sucrose. Nat. Struct. Biol. **5**, 37-46

44 Schirmer, T., Keller, T. A., Wang, Y. F. and Rosenbusch, J. P.(1995) Structural basis for sugar translocation through maltoporin channels at 3.1 Å resolution. Science. **267**, 512-514

45 Cowan, S. W., Schirmer, T., Rummel, G., Steiert, M., Ghosh, R., Pauptit, R. A., Jansonius, J. N. and Rosenbusch, J. P. (1992) Crystal structure explain functional properties of two *Escherichia coli* proteins. Nature. **358**,727-733

46 Eisele, J.L. and Rosenbusch, J.P. (1990) In vitro folding and oligomerization of a membrane protein. Transition of bacterial porin from random coil to native conformation. J. Biol. Chem. **265**, 10217-10220.

47 Ho, Y. P. and HSU, P. H. (2002) Investigating the effects of protein patterns on microorganism identification by high-performance liquid chromatography-mass spectrometry and protein database searches. J. of Chromatography. **976**, 103-111

Figure Legends

Figure 1: Elution profile and Urea SDS-PAGE of *Bps*Omp38 and *Bth*Omp38 porins.

A. Gel filtration chromatography (Sephacryl S-200® HR, Pharmacia). Proteins released from *B. pseudomallei* crude peptidoglycan in 10 mM Tris-HCl pH 8.0 containing 2% SDS and 0.5 M NaCl, were applied to a column (1.5 x 95 cm) equilibrated in 10 mM Tris-HCl, pH 8.0, containing 1% SDS and 0.5 M NaCl. Fractionation was carried out at a flow rate of 1 ml min^{-1}, and 2 ml fractions were collected. Eluted protein was measured by A_{280}. The profile for *B. thailandensis* protein was identical.

B. SDS-PAGE analysis of *Bps*Omp38 and *Bth*Omp38 proteins purified from *B. pseudomallei* under heated (U) or unheated (UH) conditions. Samples were prepared in the sample buffer containing 8 M urea at 25 °C for UH *Bps*Omp38 and UH *Bth*Omp38 or at 95 °C, 5 min for H *Bps*Omp38 and H *Bth*Omp38.

Figure 2: Immunoblots of *Bps*Omp38, *Bth*Omp38 and *E. coli* BL21 (DE3) porin.

A. Non-denatured (unheated) SDS-PAGE analysis (left) and corresponding immunoblot using anti-*Bps*Omp38 polyclonal antibodies (right). **B. Denatured** (heated) SDS-PAGE analysis and corresponding immunoblot (right). Note that because of differences in exposure times, it was not possible to carry out immunoblots of both boiled and non-boiled samples on the same gel.

Figure 3: FTIR analysis of *Bps*Omp38 and *Bth*Omp38.

Secondary derivative spectra of *Bps*Omp38 (—) and *Bth*Omp38 (••) at amide I region (1300-1800 cm^{-1}) were normalised using the IR band of Tyr (1514.2 cm^{-1}) and superimposed. IR bands: 1626.3 cm^{-1} represents β-sheets; 1561.5 cm^{-1} and 1673.7 cm^{-1} represents turns & loops; 1695.9 cm^{-1} represents anti-parallel β–sheets; 1727.4 cm^{-1} & 1740.1 cm^{-1} represent lipopolysaccharide [37].

Figure 4: Liposome-swelling assay.

A, B: Relative diffusion rates for neutral saccharides were determined by liposome-swelling assays using proteoliposomes containing various amount of M_r 110,000 protein *Bps*Omp38 **(A)** and *Bth*Omp38 **(B)** isolated from *B. pseudomallei* and *B. thailandensis*, respectively, and 2.4 µmol phosphatidylcholine and 0.2 µmol of dicetylphosphate (final volume 600 µl). The following symbols represent, in order, *L*-arabinose (○); *D*-Glucose (□); *D*-mannose (Δ); *D*-galactose (◊); *N*-acetyl glucosamine (●); *D*-sucrose (■); *D*-melezitose (▲); stachyose (♦).

C Relative permeabilities. Initial relative swelling rates for liposomes containing purified *B. pseudomallei* (Δ) and *B. thailandensis* (○) porins plotted on a logarithmic scale against the M_r of the permeating solute (abscissa). Data are shown as means ± SEM (n=3 experiments for each protein, rate for arabinose = 100%). The size-dependent swelling rates for the two porins are indistinguishable, and the straight line is a regression fit to all the data. The dashed lines indicate the 95% confidence limits of the fit. The near-limiting M_r defined as 5% relative permeability through both *Burkholderia* porins is 650 (*cf* 450 for *E. coli* porin reconstituted under the same conditions, not shown).

Figure 5: Predicted amino acid sequences of Omp38.

Purified *Bps*Omp38 and *Bth*Omp38 were subjected to capillary HPLC-ESI/MS. The amino acid sequences of tryptic peptides determined by HPLC-ESI/MS analysis are represented in bold type (uppercase and lower case), and the signal sequences are underlined. D in a box is the only amino acid in the signal sequence of *Bth*Omp38 found to be different from *Bps*Omp38.

Figure 6: Alignment of *Bps*Omp38 and *Bth*Omp38 with other outer membrane porins.

Porins were selected on the basis of a high degree of amino acid identity with Omp38. The secondary structure of *Bps*Omp38 and *Bth*Omp38 was predicted by comparison with porins of known structure (OmpF and Omp 32).

Explain texts: *Ecoli*2OmpF: OmpF porin from *Escherichia coli*; *Ecoli*1PHO: phosphoporin (PhoE) from *Escherichia coli*; *Sma*OmpC: outer membrane protein C precursor (OmpC) from *Serratia marcescens*; *Kpn*1OmpK36: osmoporin (Ompk36) from *Klebsiella Pneumoniae*; *Sty*OmpS2: outer membrane protein S2 precursor from *Salmonella typhi*; *Nme*Omp: Class 3 outer membrane porin from *Neisseria meningitidis*; *Ngo*Omp: outer membrane porin from *Neisseria gonorrhoeae*; *Ngo*Omp1: outer membrane protein I precursor from *Neisseria gonorrhoeae*; *Nsi*OmpPIB: major outer membrane protein PIB precursor (PIB porin) from *Neisseria sicca*; *Nme*PIA: major outer membrane protein P.IA precursor (PIA Class 1 protein) from *Neisseria meningitidis*; *Pce*Omp: major outer membrane porin from *Burkholderia cepacia*; *Bce*OPCP1: OpcP1 porin from *Burkholderia cepacia*; *Cac*Omp32: anion-selective porin from *Comamonas acidovorans*; *Bps*Omp38: Omp38 porin from *B. pseudomallei* ATCC23343; *Bth*Omp38: Omp38 porin from *B. thailandensis* ATCC700388.

□, β strands; ■, loops; ▥, α helix; ◎, turns

Figure 7: Predicted topologies and 3D structures of *Bps*Omp38 and *Bth*Omp38.

A. Secondary structure prediction. Trajectories of successive C_α carbons plotted against residue number for the identical predicted *B. pseudomallei* and *B. thailandensis* porins (see Methods). The Z value (scaled from 0-1) corresponds to the predicted position of each C_α carbon relative to the plane of the membrane. Values < 0.4 represent positions in periplasmic turns, values between 0.4 - 0.6 are predicted to be in transmembrane crossings, and values > 0.6 represent extracellular loops. Putative membrane crossings are defined as trajectories bounded by periplasmic and extracellular domains. 16 such membrane crossings (often with lengths compatible with a tilted β-strand) can be identified, and the corresponding external loops are labelled L1-L8.

B. 3D structure prediction of the Omp38 protein, using Swiss-Model. The representation was drawn using Swiss-pdb Viewer version 3.7b2 and built by alignment with the closest homologue (Omp32 porin from *Comamonas acidovorans*). This figure shows 16 strands and 8 loops. The longest loop (L3) (Ser^{127} to Asp^{154}) folds inside the barrel.

Table Legend

Table 1: Purification Table for Omp38 purification from both *B. pseudomallei and B. thailandensis.* The results are the means of two separate experiments for each protein.

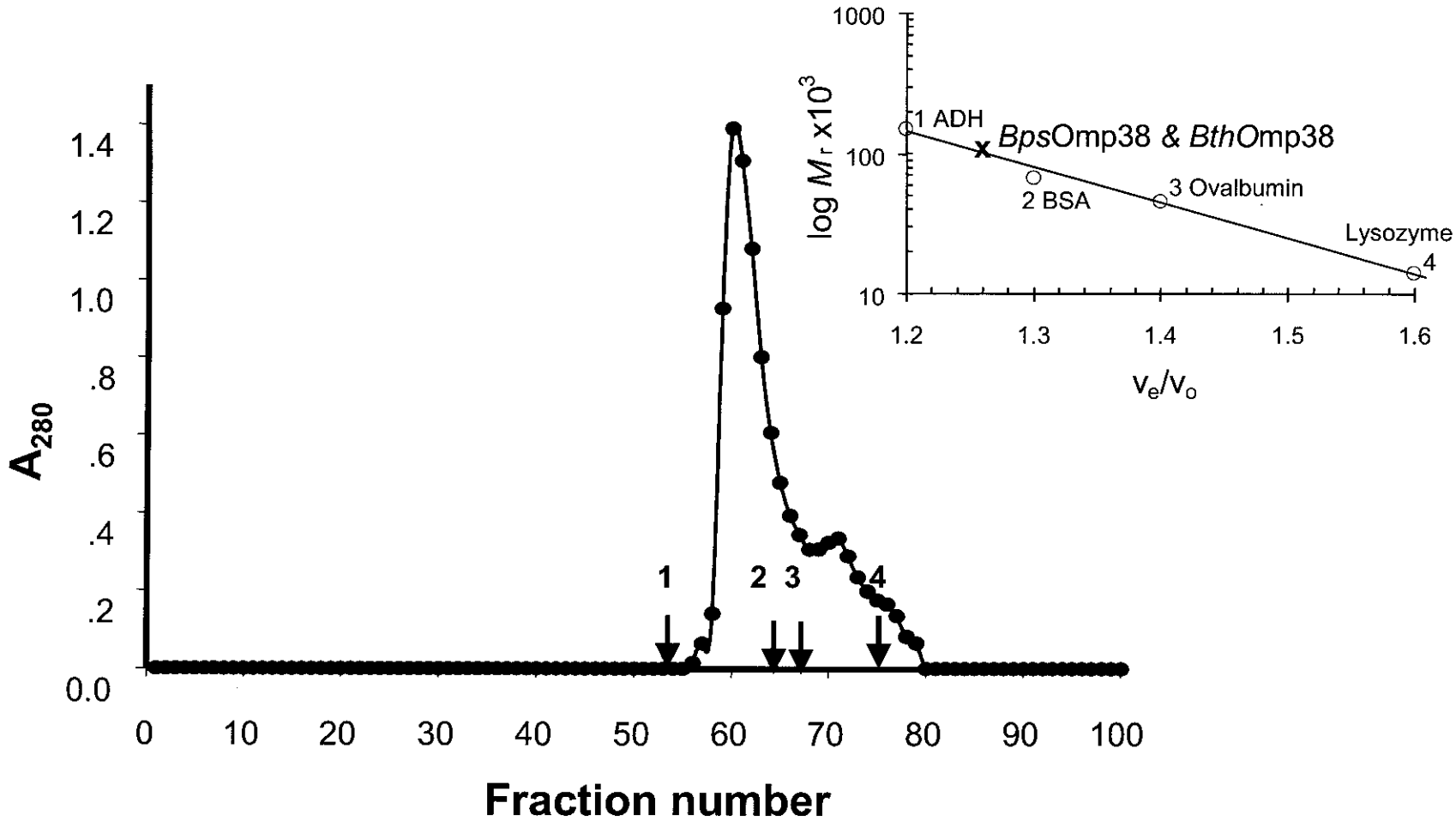
1000
100
10
log M_r x10^3
1 ADH
*Bps*Omp38 & *Bth*Omp38
2 BSA
3 Ovalbumin
Lysozyme
4
1.2
1.3
1.4
1.5
1.6
V_e/V_o
1.4
1.2
1.0
.8
.6
.4
.2
0.0
A_{280}
1
2
3
4
0
10
20
30
40
50
60
70
80
90
100
Fraction number

Figure 1A

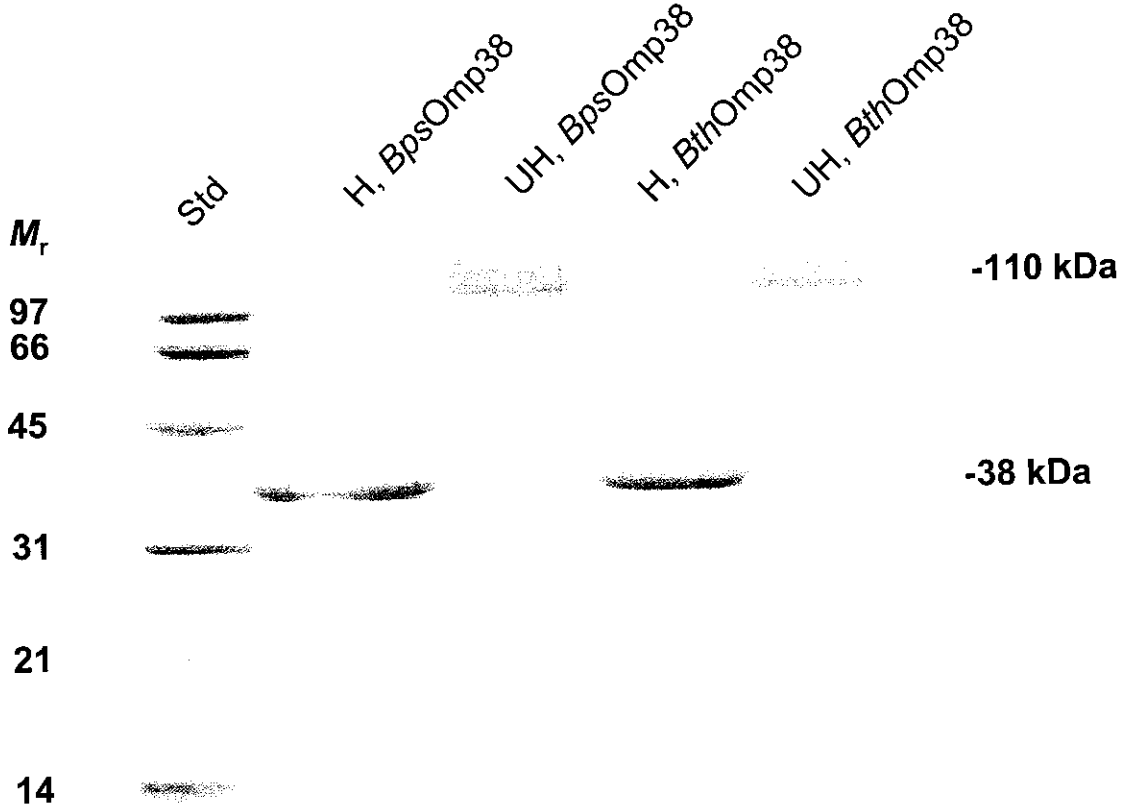
Std
H, BpsOmp38
UH, BpsOmp38
H, BthOmp38
UH, BthOmp38
Mr
97
66
45
31
21
14
-110 kDa
-38 kDa

Figure 1B

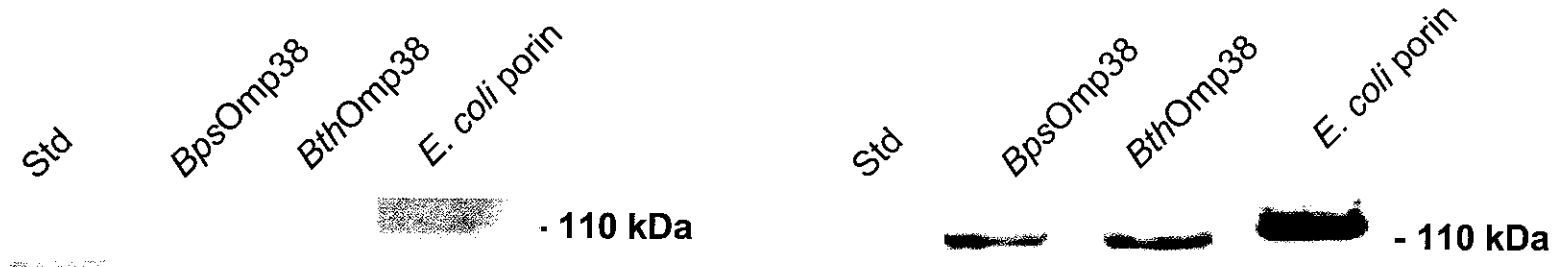
Std
BpsOmp38
BthOmp38
E. coli porin
- 110 kDa
Std
BpsOmp38
BthOmp38
E. coli porin
- 110 kDa

Figure 2A

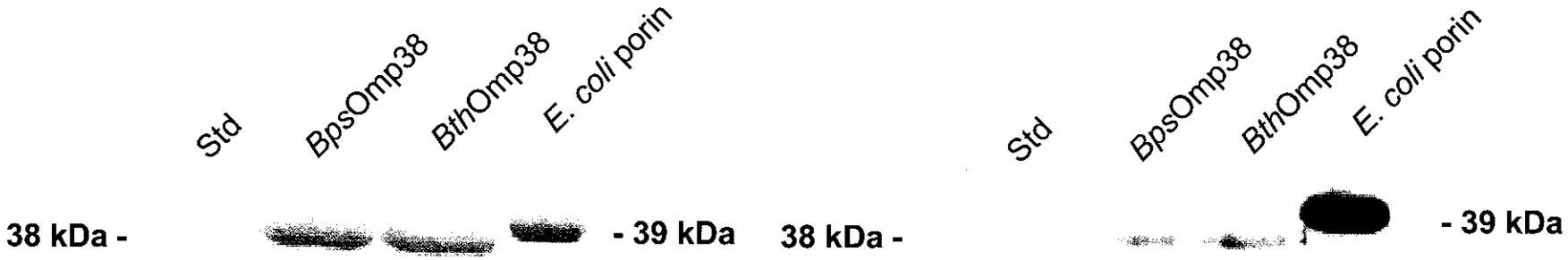
Std
BpsOmp38
BthOmp38
E. coli porin
38 kDa -
- 39 kDa
Std
BpsOmp38
BthOmp38
E. coli porin
38 kDa -
- 39 kDa

Figure 2B

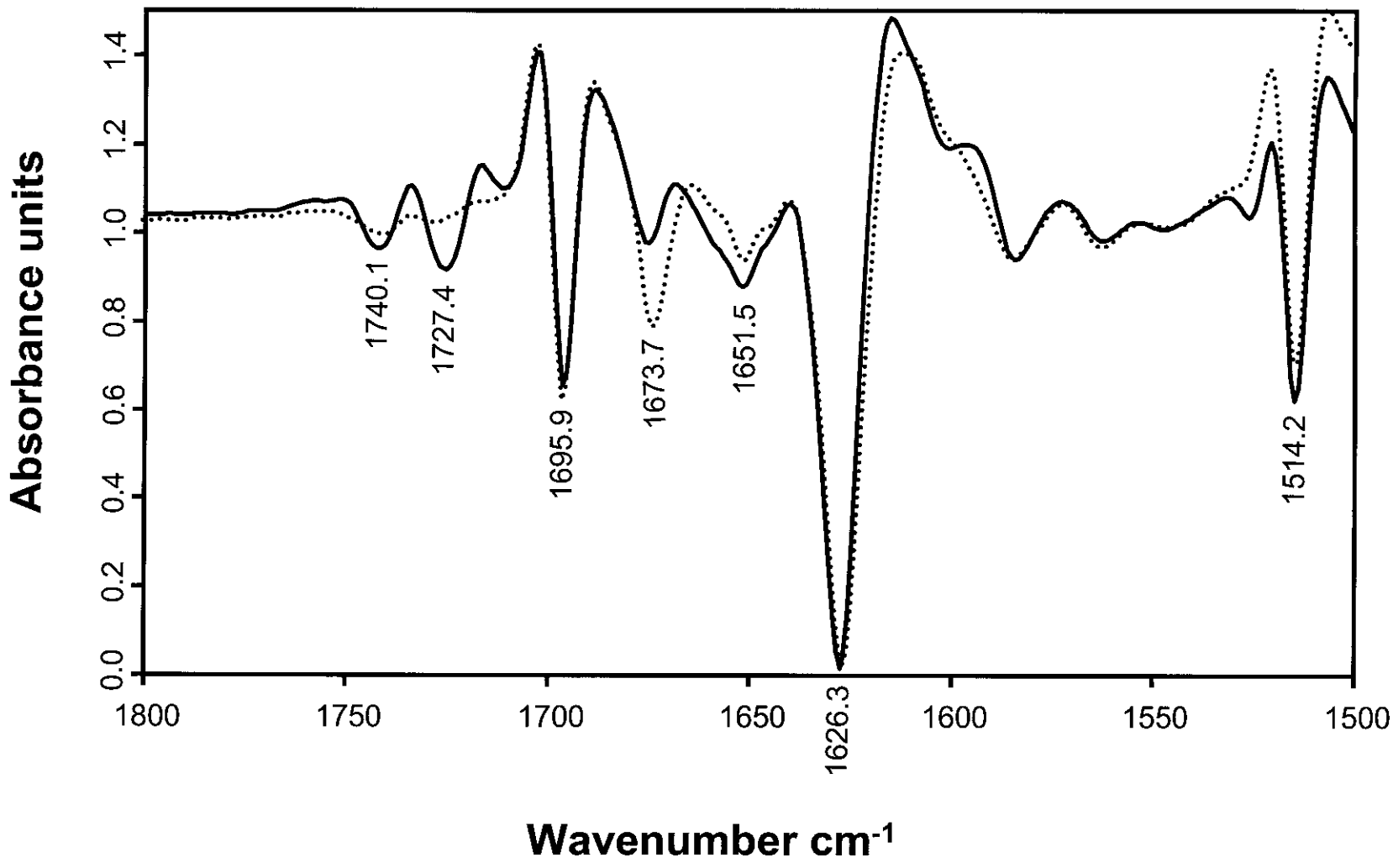
Absorbance units
0.0
0.2
0.4
0.6
0.8
1.0
1.2
1.4
1740.1
1727.4
1695.9
1673.7
1651.5
1626.3
1514.2
1800
1750
1700
1650
1600
1550
1500
Wavenumber cm-1

Figure 3

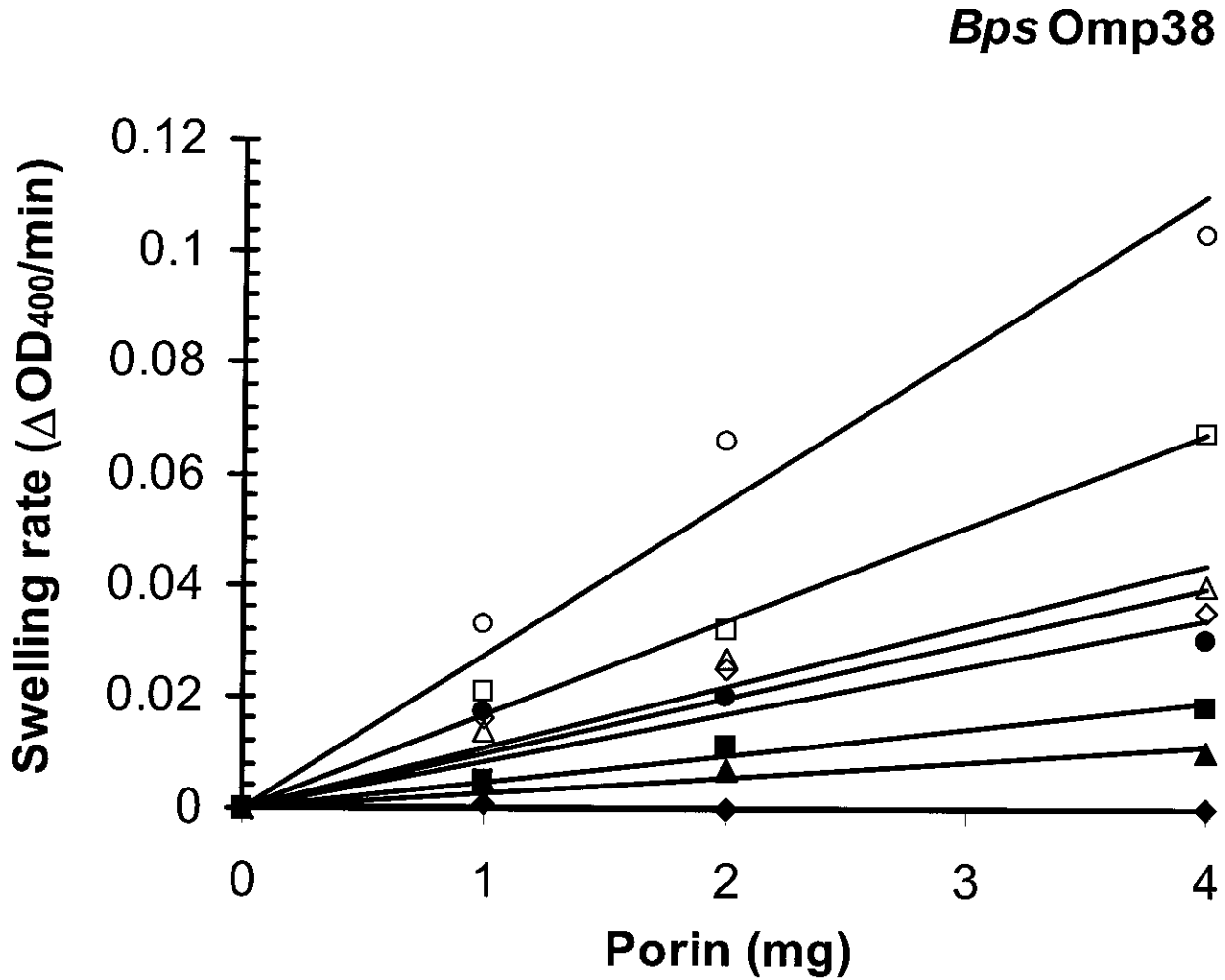
Bps Omp38
Swelling rate (ΔOD400/min)
0.12
0.1
0.08
0.06
0.04
0.02
0
0
1
2
3
4
Porin (mg)

Figure 4A

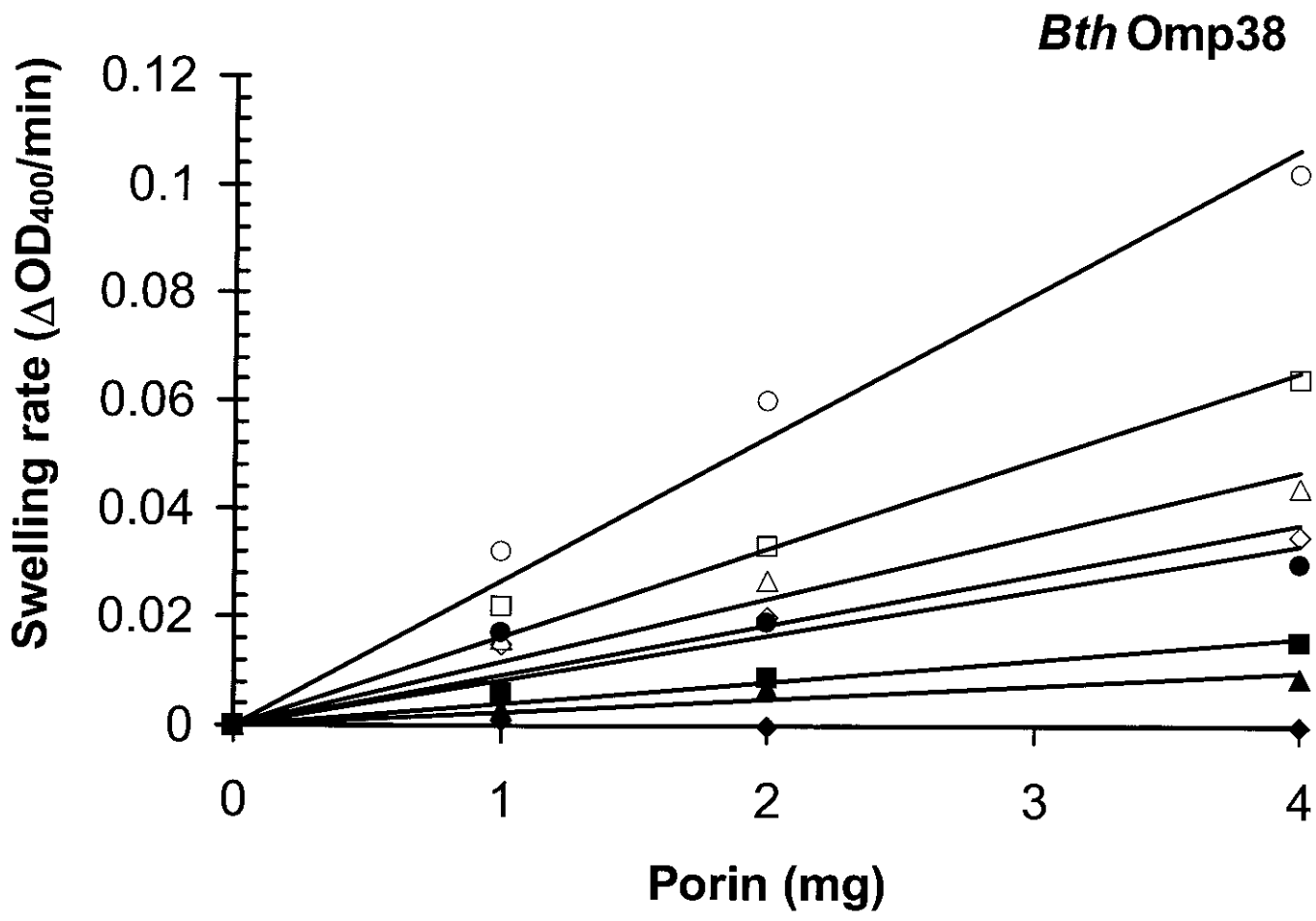
Bth Omp38
Swelling rate (ΔOD400/min)
0.12
0.1
0.08
0.06
0.04
0.02
0
0
1
2
3
4
Porin (mg)

Figure 4B

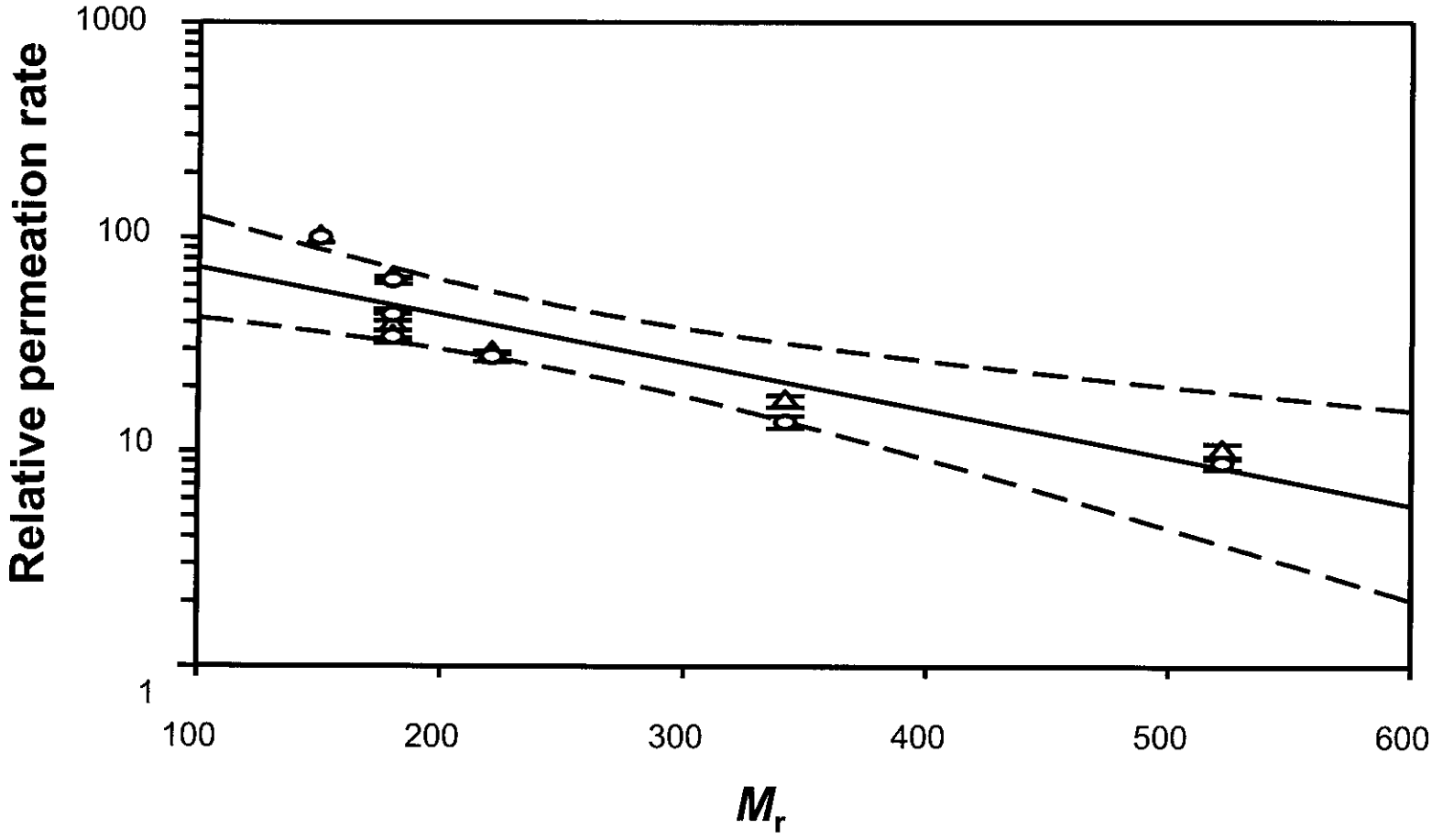
Relative permeation rate
1000
100
10
1
100
200
300
400
500
600
M_r

Figure 4C

*Bps*Omp38 and *Bth*Omp38

D

MNKTLIVAAV AASFATVAHA QSSVTLYGVL DAGITYQSNV **ATPSGSGKSL**
WSVGAGVDQS RFGLRGSEDL GGGLKaiftl esgfnigngr FNNGGGMFNR
QAFVGLSSNY GTVTLGRqyd atqdylspls atgtwggtyf ahrlnndrLN
TNGDVAVNNT VKftsanyag lqfggtysfs nnsqfannrA YSAGASYQFQ
GLKvgaaysq annaganttg atdpltgfni ggtnaasiqg rSRVYGAGAS
YAYGPLQGGL LWTQSRldnl angapttrAD NYEANVKynl tpalglgvay
tytnakANGE STHWNQVGVQ ADYALSKRtd vyaqavyqrS SKNANASIYN
GDLSTPFSTS INQTAATVGL RHRF 374

Figure 5

jure 6

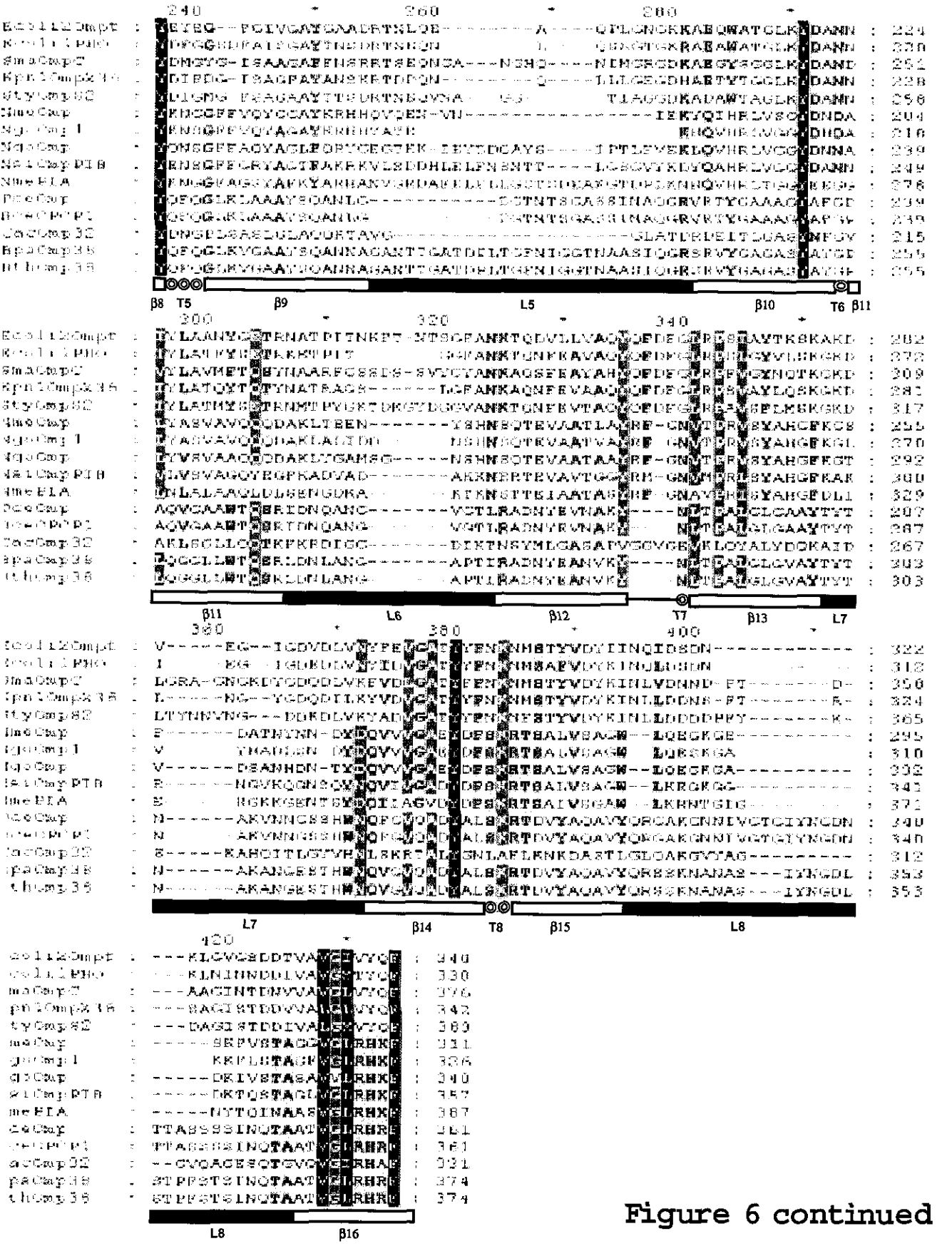

Figure 6 continued

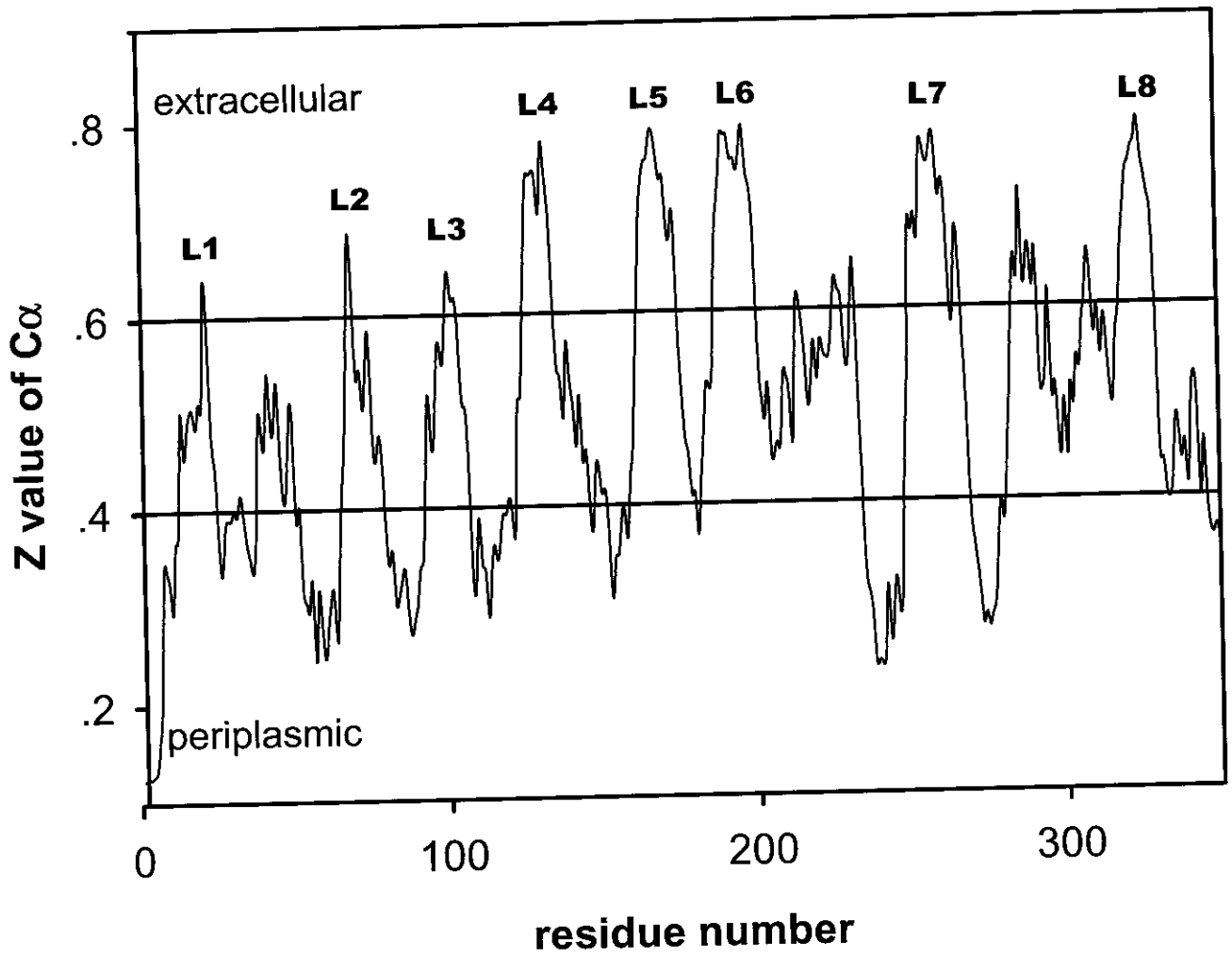
extracellular
periplasmic
L1
L2
L3
L4
L5
L6
L7
L8
.8
.6
.4
.2
0
100
200
300
Z value of Cα
residue number

Figure 7A

Top view

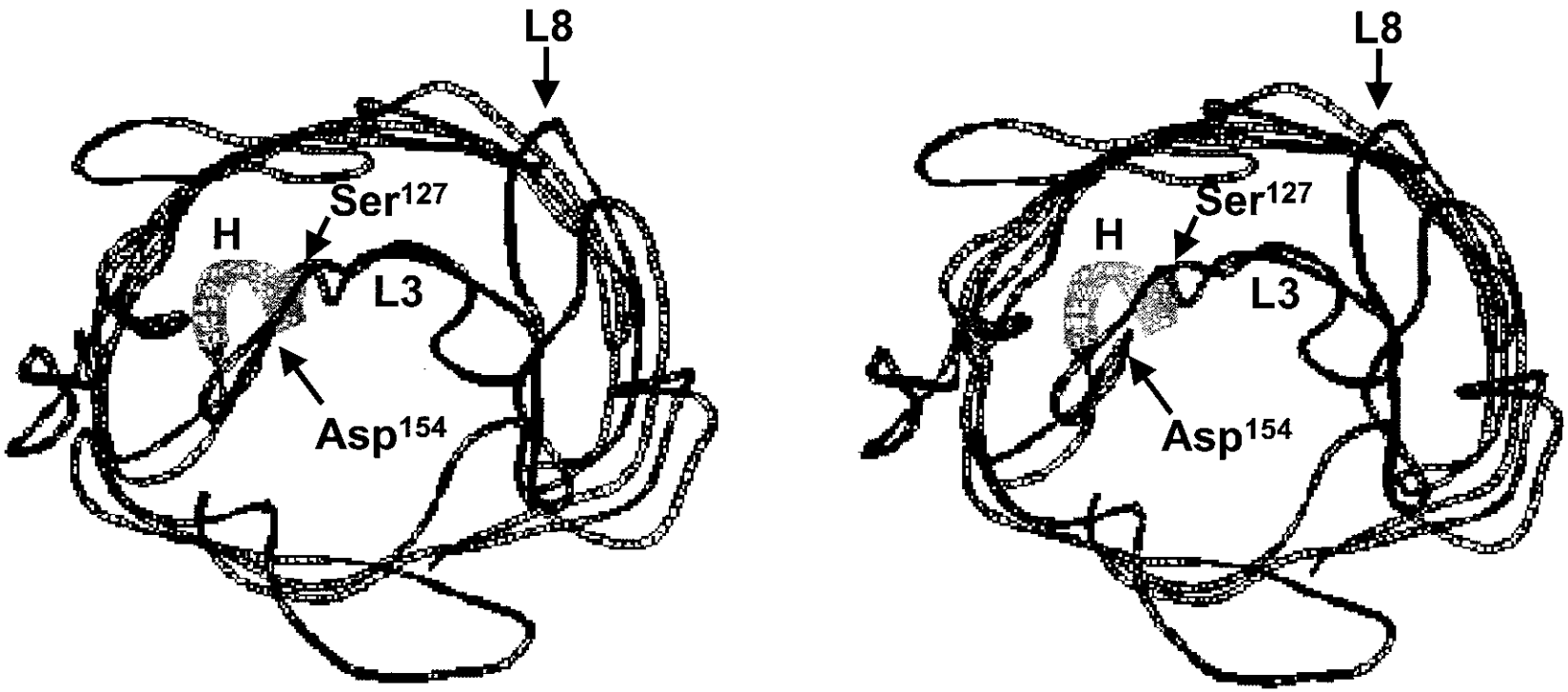

Figure 7B

Side view

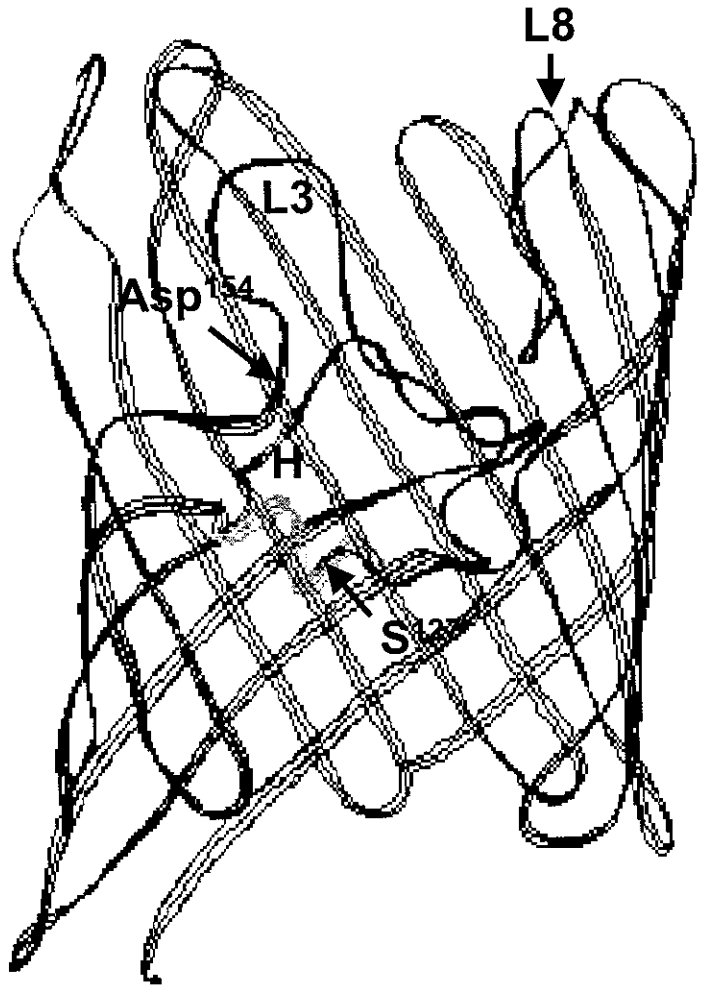

Figure 7B continued

Purification step	*B. ps* (mg)	Yield (%)	*B. th* (mg)	Yield (%)
1. Crude peptidoglycan	492.0	100	296.0	100
2. Outer membrane fraction	175.4	36	107.4	36
3. Peptidoglycan-associated fraction				
- 0.5% SDS extraction	5.4	1.1	3.4	1.1
- 2% SDS & 0.5 M NaCl extraction	5.0	1.0	3.0	1.0
4. Sephacryl S200 filtration & dialysis	0.8	0.2	0.6	0.2

Table 1